5. Discussion and Conclusion

The results of this study indicate distinctive patterns of speech and non-speech sound discrimination among autistic subjects with varying moderate to high-functioning communicative abilities and non-autistic subjects. As it can be seen from the results, using Artificial Neural Network as a method to discriminate autistic subject from non-autistic subject according to their EEG response to speech and Non-speech stimulus is feasible. These results would be statistically meaningful if more subjects were included.

This study is a pilot project trying to find a novel way to classify autism. Given the fact that MMN and P3a are two important features of Autistic ERP, it is expected that their inclusion into future studies would improve the classification accuracy.

The present results show that autistic teenagers do have different EEG response to speech and non-speech sounds from the non-autistic teenagers, not just presented in MMN and P3a, but also through the statistic features used in this ANNs approach.

The results also show that more hidden neurons (24) increase the accuracy, but at the expense of additional processing time for the ANNs to converge.

In these preliminary results, only a small number of subjects were available for this study, the confusion matrixes reveal excellent classification results. The merit of the parameters used (mean, standard deviation ...) would of course be better assessed once more subjects are recruited into this study.

Acknowledgments

The support of the National Science Foundation under grants EIA-9906600, HRD-0317692, CNS 042615, Miami Children's Hospital, and FIU's Presidential Fellowship for Ms.You is greatly appreciated.

References

[1] H. Tager-Flusberg, Strategies for conducting research on language in autism. *Journal of Autism and Developmental Disorders, 34*(1), 75-80.

[2] L. Kanner, Autistic disturbances of affective contact. *Nervous Child, 2*, 2004, 217-50.

[3] P. Heaton, B. Hermelin, and L. Pring Can children with autism spectrum disorders perceive affect in music? An experimental investigation. *Psychological Medicine, 29,* 1999, 1405- 1410.

[4] A. Klin, Young autistic children's listening preferences in regard to speech: a possible characterization of the symptom of social withdrawal. *Journal of Autism and Developmental Disorders, 21*, 1991, 29-42.

[5] R. Čeponienė, T. Lepistö, A. Shestakova, R.Vanhala, P. Alku, R. Näätänen, and K. Yaguchi, Speech-sound selective auditory impairment in children with autism: They can perceive but do not attend, *PNAS, 100*(9), 2003, 5567-5572.

[6] P. Ozand, A. Al-Odaib, H. Merza, S. Al Harbi, Autism: A review, *Journal of Pediatric Neurology, 1*(2), 2003, 55-67.

[7] N. Boddaert, N. Chabane, P. Belin, M. Bourgeois, V. Royer, C. Barthelemy, M.C. Mouren-Simeoni, A. Philippe, F. Brunelle, Y. Samson, M. Zilbovicius, Perception of complex sounds in autism: abnormal auditory cortical processing in children. *American Journal of Psychiatry, 161*, 2004, 2117–2120.

[8] R. Näätänen, The mismatch negativity: A powerful tool for cognitive neuroscience. *Ear and Hearing, 16*, 1995, 6-18.

[9] T. Lepistö, T. Kujala, R. Vanhala, P. Alkue, M. Huotilainen, R. Näätänen, The discrimination of and orienting to speech and non-speech sounds in children with autism. *Brain Research, 1066*, 2005,147 – 157.

[10] R. Ferri, M. Elia, N. Agarwal, B. Lanuzza, S.A. Musumeci, G. Pennisi, The mismatch negativity and the P3a components of the auditory event-related potentials in autistic low-functioning subjects. *Clinical Neurophysiology,114*, 2003,1671-1680.

[11] P.K. Kuhl, S. Coffey-Corina, D. Padden and G. Dawson, Links between social and linguistic processing of speech in preschool children with autism: behavioral and electrophysiological measures. *Developmental Science, 8*(1), 2005, 1-12.

[12] G. Dawson, A.N. MeltzoffOsterling, J. Rinaldi, and E. Brown, Children with autism fail to orient to naturally occurring social stimuli. *Journal of Autism and Developmental Disorders, 28*(6), 1998, 479-485.

[13] I. Cohen, An artificial neural network analogue of learning in autism. *Biological Psychiatry, 36*, 1994 5-20.

[14] L. Gustafsson, Inadequate cortical feature maps: a neural circuit theory of autism. *Biological Psychiatry, 42,* 1997, 1138-1147.

[15] L. Gustafsson and A.P. Papliński, Self-organization of an artificial neural network subjected to attention shift impairments and familiarity preference, characteristics studied in autism. *Journal of Autism and Developmental Disorders, 34*(2), 2004, 189-198.

[16] L. Fausett, "*Fundamentals of Neural Networks. Architectures, Algorithms, and Applications*" (Prentice-Hall Inc., 1994)

[17] B. Widrow and M.A. Lehr. 30 years of adaptive neural networks: perceptron, madaline, and backpropagation. *Proceedings of the IEEE, 78*(9), 1990, 1415-42.

[18] M. Adjouadi, M. Ayala, Introducing Neural Studio: An Artificial Neural Networks Simulator for Educational Purposes, *Computers in Education Journal, 14*(3), 2004, 33-40.

Proceedings of the IASTED International Conference
GRAPHICS AND VISUALIZATION IN ENGINEERING
January 3–5, 2007, Clearwater, Florida, USA
ISBN Hardcopy: 978-0-88986-625-6 / CD: 978-0-88986-627-0

CAN EEG PROCESSING REVEAL SEIZURE PREDIC

Maria T. Tito[1], Melvin Ayala[1], Ilker Yaylali[2], Mercedes Cabrerizo[1] Armando Barreto[1], I
[1]Department of Electrical and Computer Engineering, Florida Internat
10555 W. Flagler Street, Miami FL 33174, Tel: (305) 348-301
Emails: maria.tito@fiu.edu, ayalam@fiu.edu, mcabre05@fiu.edu, barretoa@fiu.edu, rishe
[2]Department of Neurology, Miami Children's Hospital
3100 South West 62nd Avenue, Miami, Fl 33155, Tel: (305) 663-8
Email: Ilker.Yaylali@mch.com

ABSTRACT

Epilepsy is characterized by an unexpected and frequent malfunction of the brain. Electrical activity in the brain has been studied for years in an attempt to predict seizures. This paper processes raw intracranial EEG recordings from different subjects in the time prior to seizure.

A set of indicators is extracted from non-overlapping scrolling windows of 1 sec duration. The objective was to identify patterns that reveal that a seizure is developing before it occurs.

While the exhaustive analysis did not detect patterns appropriate to predict a seizure, some indicators were observed to behave in time more similar independent of the subject. Similar time evolution was found for the activity and the power of the alpha and delta bands. It is also shown that the behavior of the correlation integral is somehow similar minutes before the seizure.

KEY WORDS

EEG, Epilepsy, Seizure prediction.

1. Introduction

The National Institute of Neurological Disorders and Stroke estimates that more than 2 million people in the United States have experienced an unprovoked seizure or been diagnosed with epilepsy. For about 80 percent of those diagnosed with epilepsy, seizures can be controlled with some medicines.

EEG has been studied for years in an attempt to predict seizures. Anything that disturbs the normal pattern of neuron activity can lead to seizures.

In the area of epilepsy, where the most important goal is to predict seizures, different measures have been used for years, without much success to produce reliable, prospective seizure prediction [1, 2]. This outcome is quite understandable given the challenge imposed by such a critical research endeavor. In the context of this study, many of the methods currently available in the specialized literature have been tested yielding contradictory results. In an effort to compile all methods and conduct a detailed investigation on EEG data towards seizure prediction, this

study extracts a rich s
analyzes its behavior
would reveal that
observations will be
made for future studies

In recent decades, a de
the chaotic nature of
result, non-linear dyn
these signals. Correla
common basis on wh
has been made in b
dimension oriented ana
variations including a
are being directed wit
the elusive problem
promising results ar
Nevertheless, no satisf
to date that is known
prediction tool under a

The effect of an une
Patients with epilepsy
nor do they do other t
as a seizure can occur

One goal is to enable
medicine than they cu
only when it is necess
medicine do not offer
therefore, another goa
patients to get prepare
before the seizure att
epilepsy patients may
occurrence of epilep
forecasted and clinica
stimulation or drug del
their emergence, or w
events. It is therefore
patterns that reveal tha
occurs. Having a mo
straightforward to de
epileptic subjects in ad

2. Methods

2.1. Data Collection

EEG recordings of 8 epileptic children were analyzed. Recording were performed during pre-surgical monitoring at the Miami's Children Hospital (MCH) using XLTEK Neuroworks Ver.3.0.5, an equipment manufactured by Excel Tech Ltd. Ontario, Canada. This data was collected at 500 Hz sampling frequency and filtered to remove DC and high frequency components using a 0.1-70 Hz band-pass filter. EEG recordings were processed in the time prior to seizure.

Table 1: Subjects' information

Subject	Age (years)	Sex	Number of files	Time range for each file (minutes)
1	10	Male	5	10
2	16	Male	2	10
3	3	Female	3	10
4	14	Male	2	10
5	17	Male	2	60
6	9	Male	3	60
7	11	Female	3	60
8	14	Male	6	60

The number of electrodes implanted differed from subject to subject; therefore, this study was performed on an intra-patient basis. Intracranial recordings of eight subjects were performed by using subdural strip or grid electrodes. In some cases, 4 contact depth electrodes were implanted.

2.2. Data Analysis

2.2.1. Data Preprocessing

The primary objective was to analyze all electrodes; depending on the size of the file, the last ten or sixty minutes preceding a seizure were analyzed. The size of some raw data files was higher than one gigabyte containing more than 1,800,000 samples; to that end, a software [9] was developed to split the files into readable pieces easier to handle.

Data sets used are from 8 subjects (six male, two female; age range, 3–17 years) with epilepsy in whom subdural strips and/or grid electrodes were implanted. Each subject has a different number of EEG files; the relevant information for all patients is given in Table I., including the time range of the data files. For subjects 1-4, all files extend from 10 minutes prior to seizure onset. The time interval for the other subjects was a 60 minute time range, (60 minutes prior to seizure onset).

2.2.2. Electrode Categorization

Previous studies on related matters [10] reveal that there is a tendency on the behavior of the electrodes that lead to seizure which is not given in those not leading to seizure. A portion of this research was devoted to confirm these previous findings. For this purpose, each set of electrodes was divided into three categories; those that led to seizure, those that contained interictal spikes and did not lead to seizure and those that did not contain interictal spikes and did not lead to seizure. To identify the different categories of electrodes; neurologists performed a visual inspection of the recorded data.

The analysis of data depending on these categories has been performed in this study with the only purpose of confirming observations but not with the intention of searching for patterns that could be used for seizure prediction. To make a distinction in the context of this study, we will denote the later as "category" analysis, in contrast to the "global" point of view where all measurements will be "averaged" regardless their electrode categories (as it will be shown next) for further analysis in the search for seizure advent revealing patterns.

The following groups are defined for further reference:

- Group All: grand average of feature values across all electrodes without distinction
- Group 1: Group formed by grand average of feature values of all electrodes leading to seizure
- Group 2: Group formed by grand average of feature values of all electrodes not leading to seizure
- Group 3: Group formed by grand average of feature values of all electrodes not having interictal behavior

2.2.3. Feature Extraction

Due to the high volume of information contained in the EEG raw data files, size reduction was necessary. Data files were segmented in one second time windows and features were extracted for all windows. The size of the set was thus reduced to a small number of features that are representative of the EEG. This set of features was then used for the study.

The following twelve features were considered:

- F_1: activity
- F_2: mobility
- F_3: complexity
- F_4: Average of auto correlation
- F_5: STD of auto correlation
- F_6: spectral power in the delta (less than 4 Hz) band
- F_7: spectral power in the theta (4 - 8 Hz) band
- F_8: spectral power in the alpha (8 - 13 Hz) band
- F_9: spectral power in the beta I (13 - 20 Hz) band
- F_{10}: spectral power in the beta II (20 - 36 Hz) band
- F_{11}: spectral power in the gamma (36 - 44 Hz) band
- F_{12}: correlation integral.

There are other interesting features used in EEG processing, such as the Lyapunov exponent which is a complex mathematical quantity in which the amount of chaos in the brain is measured [11]. But they were not included in the analysis because they are computationally intensive. For compensation, the correlation integral was included in the list, which is a non linear feature related to the Lyapunov exponent.

Activity, mobility, complexity are known as Hjorth parameters [12]. *Activity* A_x is simply the variance of the signal segment x and is defined as:

$$A_x = \sigma_x^2 \qquad (1)$$

Mobility Mx, is computed as the square root of the ratio of the activity of the first derivative of the signal to the activity of the (original) signal:

$$M_x = \sqrt{\frac{A_{x'}}{A_x}} = \frac{\sigma_{x'}}{\sigma_x} \qquad (2)$$

where x' represents the first derivative of the signal x.

Mobility gives a measure of deviation of the voltage changes with respect to deviation of the EEG voltage amplitude *Complexity* is defined as the ratio of the mobility of the first derivative of the signal to the mobility of the signal itself:

$$C = \frac{M_{x'}}{M_x} = \frac{\sigma_{x''}/\sigma_{x'}}{\sigma_{x'}/\sigma_x} \qquad (3)$$

where x" stands for the second derivative of the signal.

The complexity of a sinusoidal wave is unity; other waveforms have complexity values increasing with the extent of variations present in them. Complexity represents the deviation from the sine shape of the EEG signal [13].

Spectral analysis was also performed using the five recognized frequency bands of EEG activity (theta, delta, alpha, beta, and gamma). The power P_b of the frequency spectrum for these bands was computed as:

$$P_b = \int_{b_{start}}^{b_{end}} F^2(w)\,dw \qquad (4)$$

where b represents the specified frequency band and b_{start} and b_{end} its starting and ending frequencies.

Auto correlation A performs analysis in the time domain and is based on the autocorrelation function of short epochs of EEG data. The autocorrelation function is simply the expected value of a product. It is given by:

$$A = \frac{1}{N}\sum_{i=0}^{N-m-1} x_i * x_{i+m} \quad \text{for } 0 \le m \le N\text{-}1 \qquad (5)$$

Correlation integral i
in data. It is given by

$$C_{m,r} = C_r = \frac{1}{N}$$

where N is the total
segment inside the
function, and $|x_i\text{-}x_k|$ i
vector x_i used in the
embedded phase cons
a single time
following: $X_i = (x_i, x$
m is the so called en
The correlation integ
of point pairs inside a

2.2.4. Parameter Ex

In this study, the nur
from subject to subj
differently located,
regardless of the nu
location. For this
deviation (STD) of
electrodes.
Two scopes were co
option was to compu
category. Additionall
were computed af
categories together.
All calculations were
package [14].

3. Results

After computing eac
plotted for visual in
such as decreasing o
changes that could re
shows a time plot of
global features for
remaining subjects w
space reasons.

As it can be observ
could not be detecte
power, Beta II powe
hand, there is contin
STD of autocorrelati
seizure onset, there i
few seconds before
power, Theta power,
noticed that the
decrementing in mag

Fig. 2 shows a time plot of mean and standard deviation of the category features for subject # 8. Group 1, group 2 and group 3 are represented in red, blue and black, respectively. As it can be observed from the Fig. 2, some patterns stand out; for instance, there is a constant increment for the average and STD of the autocorrelation for all groups. There is also an increment in the Activity, Delta power, Theta power, Alpha power for groups 2 and 3. And surprisingly, there is a noticeable decrement in the correlation integral for group 3, which are the electrodes that do not contain interictal behavior.

Despite the observation made on Fig. 1 and Fig. 2, a close observation on the remaining subjects revealed that there are in general no patterns that show consistency in their behavior.

To enhance the study, a new measure was established in order to compute how similar each feature's behavior was across all EEG files within the subjects (intrapatient analysis). This degree of similarity allowed comparing several time series by assigning a similarity degree to the entire group. This value represents how similar time series were to each other. After extracting all features, a similarity degree was computed in order to select the most important parameters. The following equation is proposed to determine the degree of similarity of a feature whose behavior in time is described by the function *f*:

$$S = e^{-\left(\frac{1}{N}\sum_{t=1}^{N}\frac{1}{\mu_t^2}\sum_{i=1}^{M}(f_{it}-\mu_t)^2\right)} \qquad (7)$$

where f_{it} represents the value of the feature for the seizure *i* evaluated at time *t*, *M* is the number of seizures, *N* is the number of seconds in a signal and μ_t is the average of f_{it}.

Equation (8) was designed so as to yield 1.0 when all time series are identical. It considers very particular similarity criteria; however it was consistently applied to all data files thus it served well for comparison purposes. Additionally, abrupt changes in the features were analyzed by computing the first derivative of the measures and then out-thresholding it to 1.0 STD above and below mean, with the purpose of detecting pronounced peaks and valleys.
As a result, the scope of the investigation was expanded to the following time series:

- Group All (Average of features across all electrodes)
- Thresholded derivative of group All
- Group 1
- Thresholded derivative of group 1
- Group 2
- Thresholded derivative of group 2
- Group 3
- Thresholded derivative of group 3

for all features of each subject. This resulted in 16 tables for a total of 8(groups)*12(features)*2(parameters) = 192 values of similarity per subject. Rather than using the similarity for each subject, it was considered more appropriate to average the similarities for all groups and features across all subjects. This would allow making general assessments regarding which indicators behave more alike.

Tables 2 and 3 show the grand similarity per group and feature. Values above 0.5 are marked. A qualitative comparison between the results illustrated in Table 2 and 3 are provided in Table 4, which enhances all cells that showed values above 0.5 in both tables. From the comparison it can be concluded that the pair group/features that behave more alike are the following ones:

- F_1/Group All (th)
- F_6/Group All (th)
- F_8/Group 1 (th)
- F_8/Group 2 (th)
- F_8/Group 3 (th)
- F_{12}/Group All (th)
- F_{12}/Group 2 (th)
- F_{12}/Group 3 (th)

It can be observed that the Activity and Delta power for Group All (Thresholded), Alpha power for Groups 1, 2 and 3 (Thresholded) and the Correlation Integral for Group All, 2 and 3 (Thresholded) behaved more alike across all subjects.

From the observations it can be stated that features F_6, F_8, and F_{12} have a behavior distinct from the remaining features and therefore needs to be further investigated. The spectral power in the alpha band behaves very similar across all subjects for the thresholded derivatives in the three electrode groups. It is therefore important to keep an eye on these features when developing seizure prediction algorithms.

It was also noticed that the thresholded derivative of Group All has similarity above 50%. It is believed that refining this indicator will lead to further findings.

It is interesting to note that the results confirm pervious findings [10] related to the importance of the correlation integral (F_{12}) in discriminating the three groups of electrodes in real-time classification.

4. Conclusion

In this study, a total of 26 EEG files recorded at least 10 minutes before a seizure were scrutinized from 12 different points of view called features. An extensive observation did not detect any significant patterns occurring prior to seizure onset. However, further examination yielded an interesting outcome about activity, power of the alpha and beta bands and correlation integral: these three features have a more similar behavior across all subjects than the remaining features. This was proven with the introduction of a new indicator called similarity that was consequently utilized to obtain a rough idea of how similar time series develop in time.

At this stage of the study it was not possible to use the similarity results for seizure prediction, but the authors believe that predictive patterns may be found with proper variations and/or combinations of those features.

Acknowledgments

The support of the National Science Foundation and the Office of Naval Research under grants EIA-9906600, HRD-0317692, CNS 042615, N00014-99-1-0952, and Miami Children's Hospital is greatly appreciated.

References

[1] Y. Lai, M.F. Harrison, M.G. Frei and I. Osorio, Inability of Lyapunov Exponents to predict epileptic seizures, *Physical Review Letters, 91*(6), 2003.

[2] L.D. Iasemidis, A. Barreto, R.L. Gilmore, B.M. Uthman, S.A. Roper and J.C. Sackellares, Spatiotemporal evolution of dynamical measures precedes onset of mesial temporal lobe seizures, *Epilepsia*, vol. 35 (Suppl 8), pp. 133, 1994.

[3] G.W. Frank, T. Lookman, M.A.H. Nerenberg, C. Essex, J. Lemieux and W. Blume, Chaotic time series analyses of epileptic seizures , *Physica D, 46,* 1990,427-438.

[4] A. Barreto, J. C. Principe and S. A. Reid, STL: A spatio-temporal characterization of focal interictal events, *Brain Topography, vol. 5, No. 3,* Human Sciences Press, New York, 1993, 215-228.

[5] M.R. Guevara, Chaos in electrophysiology, *concepts and techniques in bioelectric measurements: Is the medium carrying the Message?* edited by LeBlanc, A-R, Billette, J., Editions de l'Ecole Polytechnique de Montreal, Montreal, 1997. pp. 67-87,

[6] I. Yaylali, H. K
seizures from small s
System Theory, *P I*
1996, 743-751.

[7] A. Bezerianos,
dependent Entropy E
following brain is
Engineering, 31, 200

[8] J. Martinerie, C
Epileptic seizures c
analysis, *Nat. Med, 4,*

[9] Software devel
Technology and
http://www.cate.fiu.e

[10] M. Cabrerizo,
Pattern extraction in
detection of electrod
Sciences Instrumenta
248.

[11] J.C. Sackellares,
Chaovalitwongse, an
temporal pattern pr
prediction, U.S. Pat
(Attorney Docket No

[12] B. Hjorth,(1970
properties, *Electro*
Neurophysiology 29,

[13] R. C. Gonzalez,
digital image proce
Company, 1993).

[14] W. J. Palm, *Intr*
with 6.5 update wi
graphics, and
Science/Engineering

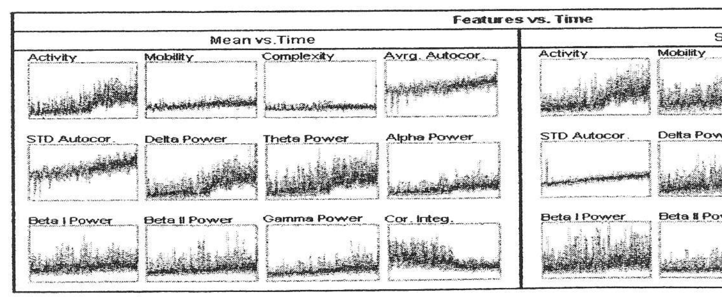

Figure 1: Mean and standard deviation of global features (Group All) over time fo

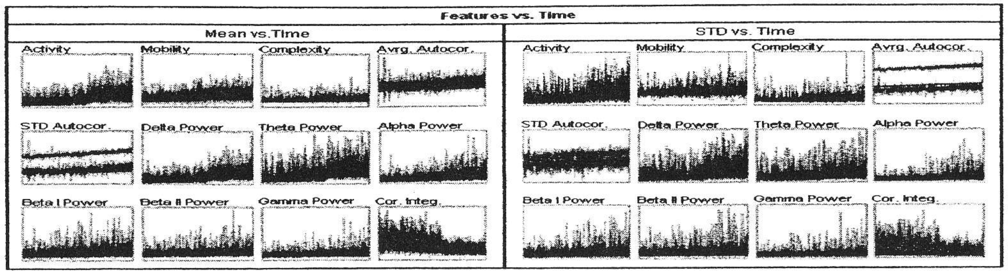

Figure 2: Mean and standard deviation of the category features (Group1, 2, and 3) over time for subject # 8, seizure # 2.

Table 2: Grand similarity of the average parameter per group and feature

Scope	Features											
	F1	F2	F3	F4	F5	F6	F7	F8	F9	F10	F11	F12
Group All	0	0	0	0.06	0.05	0	0	0	0	0	0	0
Thresholded derivative of group All	0.60	0.41	0.52	0.25	0.27	0.72	0.39	0.64	0.52	0.39	0.52	0.75
Group 1	0	0	0	0.07	0.06	0	0	0	0	0	0	0
Thresholded derivative of group 1	0.41	0.28	0.27	0.38	0.5	0.41	0.29	0.52	0.28	0.27	0.53	0.64
Group 2	0	0	0	0.07	0.02	0	0	0	0	0	0	0
Thresholded derivative of group 2	0.41	0.32	0.27	0.38	0.5	0.41	0.29	0.52	0.28	0.27	0.53	0.64
Group 3	0	0	0	0.07	0.05	0	0	0	0	0	0	0
Thresholded derivative of group 3	0.41	0.28	0.27	0.38	0.5	0.41	0.29	0.52	0.28	0.27	0.53	0.64

Table 3: Grand similarity of the STD parameter per group and feature

Scope	Features											
	F1	F2	F3	F4	F5	F6	F7	F8	F9	F10	F11	F12
Group All	0	0	0	0.09	0.09	0	0	0	0	0	0	0.11
Thresholded derivative of group All	0.51	0.52	0.27	0.39	0.41	0.62	0.39	0.27	0.43	0.57	0.38	0.75
Group 1	0	0.09	0	0	0	0	0.05	0	0.09	0	0	0.11
Thresholded derivative of group 1	0.29	0.63	0.25	0.5	0.27	0.29	0.16	0.52	0.28	0.52	0.25	0.75
Group 2	0	0	0	0.04	0	0	0	0	0	0	0	0
Thresholded derivative of group 2	0.29	0.63	0.25	0.5	0.27	0.29	0.16	0.52	0.28	0.52	0.25	0.75
Group 3	0	0	0	0.08	0.09	0	0	0	0	0	0	0.11
Thresholded derivative of group 3	0.29	0.63	0.25	0.50	0.27	0.29	0.16	0.52	0.28	0.52	0.25	0.75

Table 4: Qualitative comparison of Tables 2 and 3. Cells with both values greater than or equal to 0.5 are grayed and marked with a cross (X).

Scope	Features											
	F1	F2	F3	F4	F5	F6	F7	F8	F9	F10	F11	F12
Group All												
Thresholded derivative of group All	X					X						X
Group 1												
Thresholded derivative of group 1								X				X
Group 2												
Thresholded derivative of group 2								X				X
Group 3												
Thresholded derivative of group 3								X				X

Proceedings of the IASTED International Conference
GRAPHICS AND VISUALIZATION IN ENGINEERING
January 3–5, 2007, Clearwater, Florida, USA
ISBN Hardcopy: 978-0-88986-625-6 / CD: 978-0-88986-627-0

ON THE SECURITY OF A FRAGILE DIGITAL IMAG SCHEME

Jun Sang[1], Mohammad S. Alam[2], and Xiaohong Z
[1] School of Software Engineering, Chongqing University, Chongq
[2] Department of Electrical and Computer Engineering, University of South Ala
[3] Department of Computer Science and Engineering, Chongqing University,
Email: jsang@cqu.edu.cn

ABSTRACT
In this paper, the security of a fragile digital watermarking for image tamper detection and recovery proposed in Reference 1 is analyzed. It is shown that the secret key for watermark embedding and detection can be easily obtained by exhaustive search, while keeping the number of the necessary exhaustive searches small. Therefore, one may counterfeit watermarks successfully, resulting in incorrect authentication. The possible solutions for such problems are suggested in this paper.

KEY WORDS
Fragile watermarking, tamper detection, tamper recovery, security

1. Introduction

Nowadays, digital multimedia are widely used for various applications. Since digital multimedia can be modified easily and imperceptibly without any trace of manipulations [2], the authenticity/integrity becomes an important issue for digital multimedia. To address this problem, various digital watermarking based techniques are proposed [2, 3]. For image authentication, usually a fragile/semi-fragile watermark is embedded in an image. Any modifications to the watermarked image can be detected by the embedded watermark. Fragile watermark rejects any image manipulations, either incidental or malicious. Semi-fragile tolerates some normal image processing manipulations, such as JPEG compression, while rejects any other manipulations or malicious attacks [2].

A block-based fragile image watermarking scheme was proposed in Reference 4, where the host image is partitioned into non-overlapping blocks and a hash based watermark, calculated from the seven most significant bits (MSBs) of each block, is embedded into the least significant bits (LSBs) of the same block. The watermark detection and image authentication are conducted by verifying each block individually, i.e., the watermark embedding and detection for each block are independent from the other blocks within the image [5, 6].

By utilizing the blockwise independent authentication feature of the block-based fragile image watermarking,

Holliman et al. [5]
attack, which can
authentication when
same keys can be
generated from the
VQ attack problem
proposed [5, 6].

Recently, Lin
method for image
approach uses simpl
and detection, and
structure for wate
accuracy of tamper
some tampered regi

However, the s
insecure because the
and detection can
watermark counterf
the security problem
and suggest the poss

2. Overview

The watermarking
involves three step
detection for tamp
recovery.

2.1 Watermark Em

Consider a grayscale
is a multiple of four
embed watermark:

Step 1. Divide t
blocks
$N = M /$
blocks with
left to right

Step 2. To recover
of the block
Therefore,
correspond

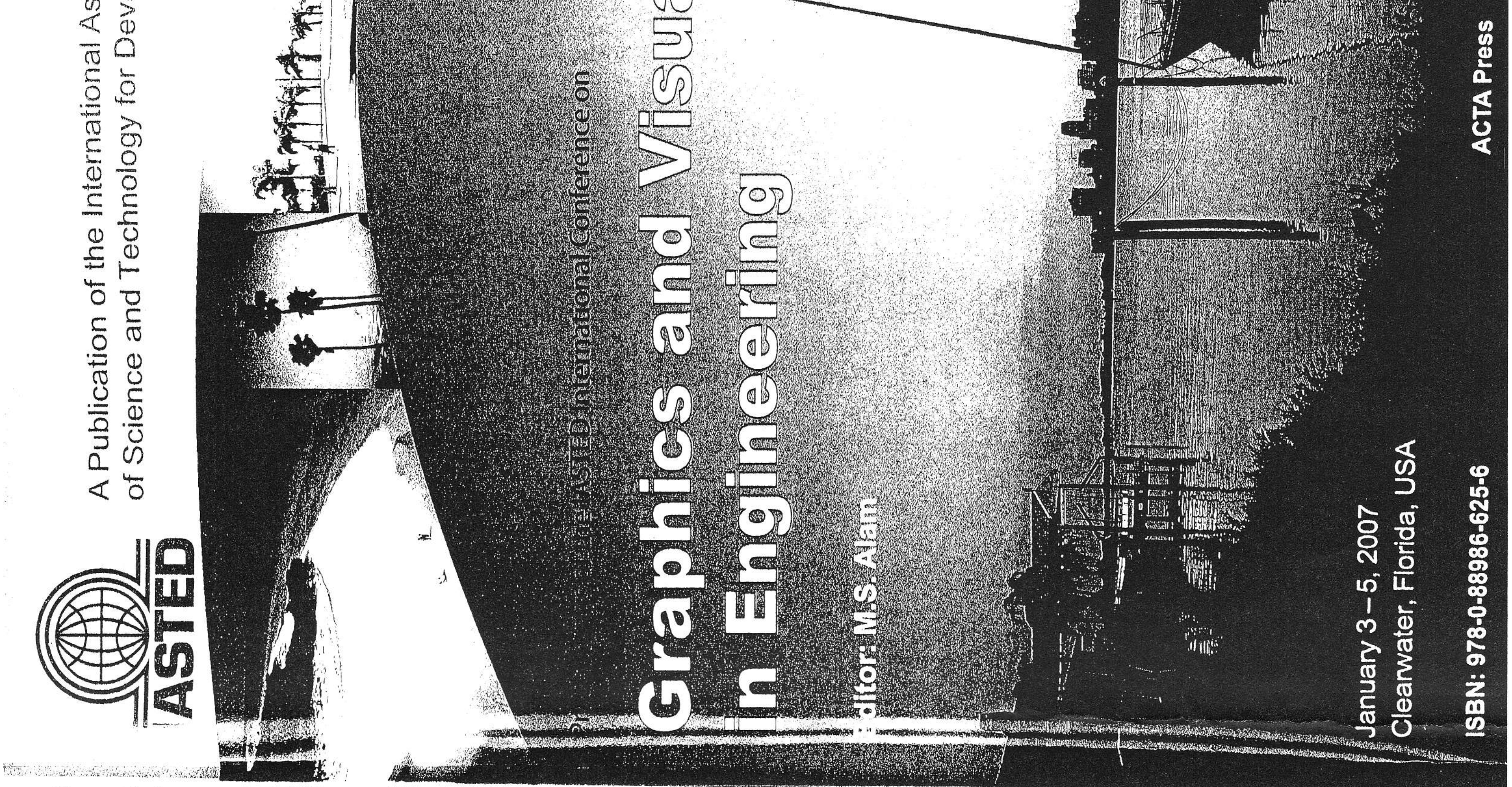

Graphics and Visualization in Engineering Editor: M.S. Alam ISBN: 978-0-88986-625-6 562

Proceedings of the IASTED International Conference on **Graphics and Visualization in Engineering**, held January 3 – 5, 2007, Clearwater, Florida, USA.

SPONSOR
The International Association of Science and Technology for Development (IASTED)
- Technical Committee on Graphics
- Technical Committee on Visualization

EDITOR
M.S. Alam – University of South Alabama, USA

KEYNOTE SPEAKER
T.K. Shih – Tamkang University, Taiwan

TUTORIAL PRESENTER
A. El-Saba – University of South Alabama, USA

For each IASTED conference, the following review process is used to ensure the highest level of academic content. Each full manuscript submission is peer reviewed by a minimum of two separate reviewers on the International Program Committee/Additional Reviewers list. The review results are then compiled. If there are conflicting reviews, the paper is sent to a third reviewer.

ACTA Press
P.O. Box 5124
Anaheim, CA 92814–5124
USA

ACTA Press
B6, Suite #101, 2509 Dieppe Ave SW
Calgary, Alberta T3E 7J9
Canada

ACTA Press
P.O. Box 354
CH–8053 Zurich
Switzerland

Publication Code: 562

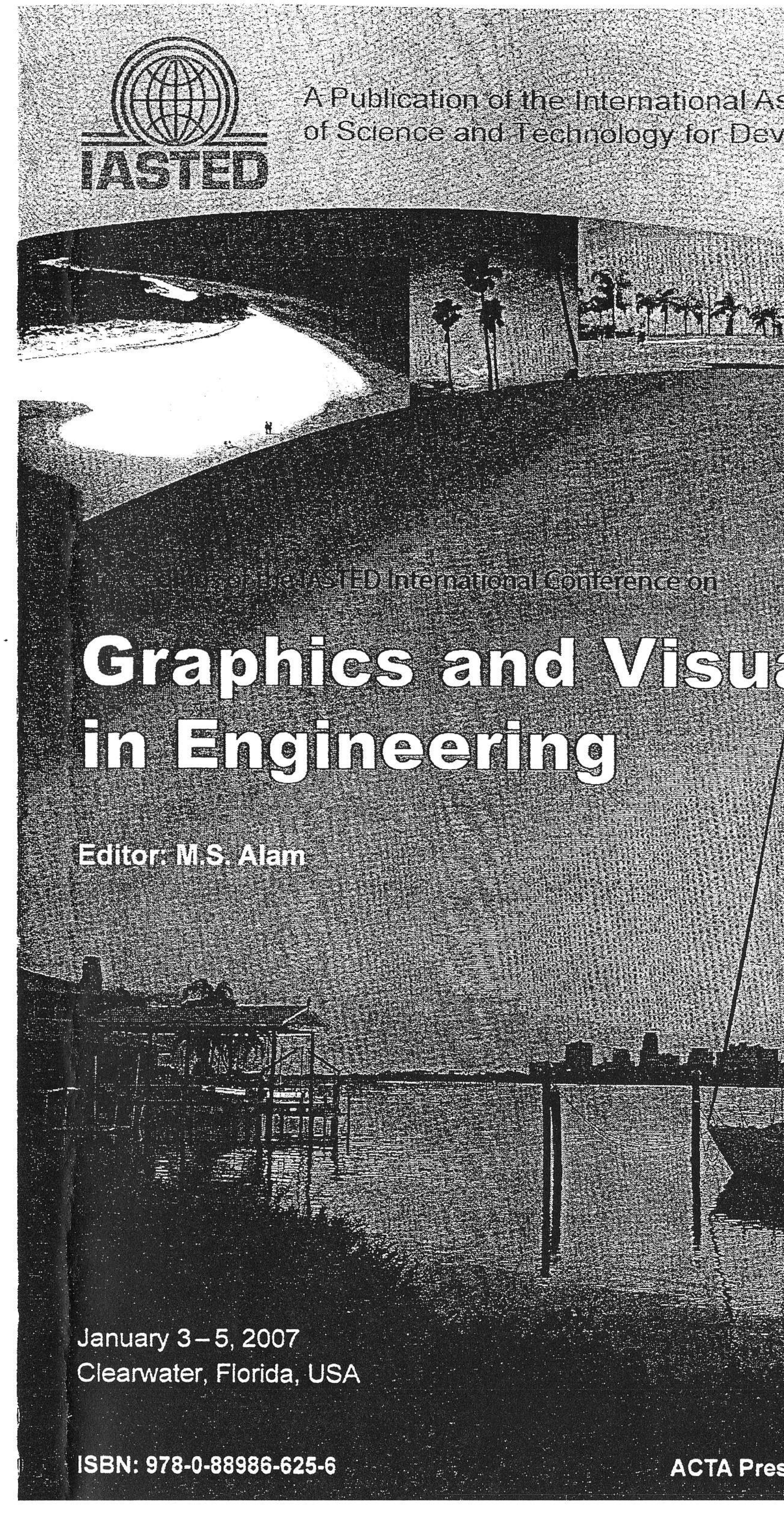

$$\begin{aligned} \mathrm{comm}_{\mathrm{Maxwell}}(n) &= [A, \partial/\partial t\ A] / \sqrt{n} \\ &= 0 / \sqrt{n} \\ &= 0 \end{aligned} \tag{11}$$

We are interested in the limiting case

$$\lim_{n \to \infty} (\mathrm{comm}_{\mathrm{QED}}(n) - \mathrm{comm}_{\mathrm{Maxwell}}(n)) = 0 \tag{12}$$

For a system that has a very large number of photons, the quantum commutator behaves like the classical commutator, demonstrating that the limiting case of QED is Maxwell's equations. In most applications the number of photons actually is quite large and so the system behaves classically. But the quantum nature of the photon is always present, and is even evident in certain macroscopic systems (like the photoelectric effect), where Maxwell's equations cannot begin to explain the phenomenon.

How large is large for the number of photons? In the visible spectrum, red light has a wavelength λ of roughly

$$\lambda \sim 6 \times 10^{-7} \mathrm{m}$$

The energy $\mathcal{E}$ (in joules J) of a single "red" photon is

$$\mathcal{E} = h\frac{c}{\lambda} = 3 \times 10^{-19} J$$

Using a light source with power of 1 watt (1 J/sec), the number n of photons emitted per second is $1/\mathcal{E}$, or about 3×10^{18}. So even in a dimly lit scene, we expect a conventional (classical) renderer to produce accurate. That comes as no surprise; the point here is that we can quantify why classical illumination is good enough.

In order for the quantum field properties of photons in a rendered scene to make a difference, we must consider a situation where there is only a small number of photons. This can occur if the time interval for the light to be collected must be very small; or the light source is very dim; or the illuminated volume is very large so the photon density is low; or the rendered volume is a very small subset of the total space, containing only a few localized photons; or the wavelength of the light is very short but energetic (which means rendering a scene illuminated by gamma rays).

5. Conclusion

We summarized the essentials of quantum electrodynamics (QED) that are needed to relate it to classical electrodynamics. In brief, the photon states form a Fock space and are represented by linear combinations of kets and are acted on by a quantum field operator *A* defined via the least action together with a commutator relation. When the number of photons is large, the effect of the quantum commutator is negligible, and it asymptotically approaches the classical commutator for the vector potential A. It is in this sense that QED approaches classical electrodynamics as presented in Maxwell's equations.

Acknowledgments

This work was supported by NSF CCF #0430954 "Mathematical Foundations of Algorithms for Data Visualization." The authors gratefully acknowledge improvements suggested by the reviewers.

References

[1] Aleksandr I. Akhiezer and Vladimir B. Berestetskii, *Elements of quantum electrodynamics* (Chapter 3), translated from the Russian *Kvantovaya elektrodinamika* by the Israel Program for Scientific Translations, Jerusalem (London: Oldbourne Press, 1962).

[2] Barry G. Becker and Nelson L. Max, "Smooth transitions between bump rendering algorithms," *Proceedings of ACM SIGGRAPH 1993*, pp. 183-190, 1993.

[3] P. Beckmann and A. Spizzichino, *The scattering of electromagnetic waves from rough surfaces* (Pergamon Press, 1963).

[4] Jim Blinn, *Jim Blinn's corner: dirty pixels* (Morgan Kaufmann Publishers, Inc., 1998).

[5] Brian Cabral *et al.*, "Bidirectional reflection functions from surface bump maps," *Proceedings of ACM SIGGRAPH 1987*, pp. 273-281, 1987.

[6] Alexander L. Fetter and John D. Walecka, *Quantum theory of many-particle systems* (McGraw-Hill, 1971).

[7] Richard Feynman *et al.*, *The Feynman lectures on physics*, Volume 2: *the electromagnetic field* (Chapters 18-20) (Addison-Wesley, Inc., 1964).

[8] Andrew Glassner, *Principles of digital image synthesis* (Morgan Kaufmann, Inc., 1995).

[9] Jay S. Gondek *et al.*, "Wavelength dependent reflectance functions," *Proceedings of ACM SIGGRAPH 1994*, pp. 213-220, 1994.

[10] Michael Peskin, *An introduction to quantum field theory* (Harper Collins 1995).

[11] David Griffiths, *Introduction to electrodynamics* (Chapter 10), 3rd Ed. (Prentice-Hall, Inc., 1999).

[12] Roy Hall, "Comparing spectral color computation methods," *IEEE computer graphics & applications*, 19(4), 1999, 36-46.

[13] John D. Jackson, *Classical electrodynamics* (John Wiley & Sons, 1975).

[14] Henrik W. Jensen and Niels J. Christensen, "Photon maps in bidirectional Monte Carlo ray tracing of complex objects," *Computers and graphics*, 1995, 19(2), 215-224

[15] James Kajiya, "Anisotropic Reflection Models," *Proceedings of ACM SIGGRAPH 1985*, pp. 15-21, 1985.

[16] James Kajiya, "The Rendering Equation," *Proceedings of ACM SIGGRAPH 1986*, pp. 143-150, 1986.

[17] Leonard Mandel and Emil Wolf, *Optical coherence and quantum optics* (chapter 10) (Cambridge University Press, 1995).

[18] Franz Mandel and Graham Shaw, *Quantum field theory* (Wiley, 1993).

[19] James C. Maxwell, *A treatise on electricity and magnetism*, Vol. 1, unabridged 3rd ed. (Dover, 1991).

[20] Hans P. Moravec, "3-D graphics and the wave theory," *Proceedings of ACM SIGGRAPH 1981*, pp. 289-296, 1981.

[21] Mark S. Peercy, "Linear color representations for full spectral rendering," *Proceedings of ACM SIGGRAPH 1993*, pp. 191-198, 1993.

[22] P. Poulin and Alain Fournier, "A model for anisotropic reflection," *Proceedings of ACM SIGGRAPH 1990*, pp. 273-282, 1990.

[23] J. Ian Richards and Heekyung K. Youn, *Theory of distributions: a nontechnical introduction* (Cambridge University Press, 1990).

[24] L. H. Ryder, *Quantum field theory* (Cambridge University Press, 1996).

[25] David C. Tannenbaum *et al.*, "Polarization and birefringency considerations in rendering," *Proceedings of ACM SIGGRAPH 1994*, pp. 221-222, 1994.

[26] Paul Teller, *An interpretive introduction to quantum field theory* (Princeton University Press, 1995).

[27] Kenneth Torrance and Ephraim Sparrow, "Theory for off-specular reflection from rough surfaces," *Journal of the Optical Society of America*, 57, 1967, 1105-1114.

[28] Stephen H. Westin *et al.*, "Predicting reflectance functions from complex surfaces," *Proceedings of ACM SIGGRAPH 1992*, pp 255-264, 1992

[29] Lawrence B. Wolff and David J. Kurlander, "Ray tracing with polarization parameters," *IEEE computer graphics and applications*, 10(6), 1990, 44-55.

AUTHOR INDEX
GVE 2007